*33rd EPS Conference on Plasma Phys. Rome, 19 - 23 June 2006 ECA Vol.**30I**, O-2.012 (2006)*

X-ray and Ion Debris Impact on the First Wetted Wall of IFE Reactor

S.A. Medin[1], M.M. Basko[2], Yu.N. Orlov[3] and V.M. Suslin[3]

[1]*Institute for High Energy Densities, Moscow, Russia*
[2]*Institute for Theoretical and Experimental Physics, Moscow, Russia*
[3]*Keldysh Institute for Applied Mathematics, Moscow, Russia*

Introduction. Here we consider a heavy-ion-fusion concept based on a cylindrical target whose length conforms to the range of heavy ions. The target is a cylindrical shell of lead filled with the DT-fuel ice. It is axially irradiated by a hollow ion beam, formed by fast rotation of the pointed beam. The implosion of the shell compresses the DT fuel. The effective performance of the target is achieved by space and time profiling of the beam pulse. The target output is computed by DEIRA-4 code [1], a one-dimensional three-temperature Lagrangian code.

The target chamber design and performance is determined by deposition of target X-rays, neutrons and ions in the chamber gases and structures, vaporization and condensation of the first wall material, generation of dynamic thermal stresses in the blanket walls. The previous design studies of a reactor chamber for heavy ion inertial fusion energy [2] show that a conservative wetted wall design can be well accepted. The protection of the first wall is provided by a thin liquid lead film. In this paper the target output and deposition of target X-rays, neutrons and ions in the evaporating liquid film at the first wall are simulated.

Target performance. The target compression and burn is computed with the DEIRA-4 code, which includes diffusion of radiation and of fast ions (in a single-energy-group approximation), kinetics of nuclear reactions, heating rates by neutrons and by fast heavy ions. The equation of state approximates realistic properties of materials in the region of strong coupling. The mathematical model, the discretization scheme and the

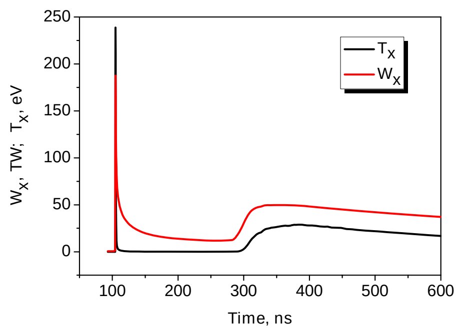

Fig.1.Time dependence of the temperature T_x and of the total power W_x of the X-rays emitted by the external surface of the expanding target.

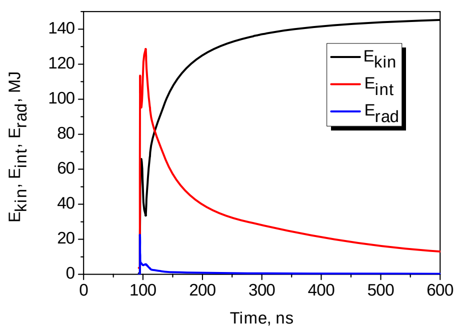

Fig.2. Time dependences of the kinetic energy E_{kin}, the internal energy E_{int} and the radiation energy E_{rad}.

algorithm of computations are described in ref.[2].

The target dimensions are chosen as follows: the length is 0.64cm, the fuel cylinder radius is 0.112cm and the target radius is 0.4cm. The masses of the lead shell and the DT fuel are equal to 3.35g and 5.7mg respectively. The target is irradiated by the lead ions of 100GeV energy. The total beam energy amounts to 6.4MJ profiled in 75ns interval with maximum of 525TW for the final stage of the pulse. The fuel burn yields 741MJ of the fusion energy with the following partition: 16MJ in the X-rays, 149MJ in the target debris, and 576MJ in fast neutrons.

The fusion flare occurs at approximately 95ns after the ion beam starts irradiating the target. The fuel burn produces a neutron pulse of 100ps FWHM. In Fig.1 the time dependence of the emitted X-ray power and temperature are plotted. It is seen that at t=104ns an X-ray prepulse, the first narrow peak, appears. The X-ray prepulse is caused by the arrival at the target surface of the shock launched by the fuel flare; its FWHM equals 500ps. The main X-ray pulse emerges at $t \approx 300$ns. It has quite long duration with FWHM of 360ns and relatively low amplitude of 27.7 TW. Such a history of X-ray generation is due to a large optical thickness of the massive lead target shell, which substantially alleviates the impact on the first chamber wall.

In Fig.2 the time dependence of the three main components of the target energy is presented. The conversion of internal and radiation energies into the kinetic energy is manifested. A dip on the E_{in} and E_{kin} curves, which occurs between the fusion flare and the shock arrival at the target surface, is caused by the wave reflection on the non-uniform density distribution in the target shell.

X-ray impact on the liquid wall. The reactor chamber first wall has the radius of 5m. The first wall is coated by the lead liquid film of 2mm thickness. For description of the liquid film response to X-ray deposition a one-dimensional spherically-symmetrical one-temperature approximation is used. Moderate energy density physics, vaporization and thermal conduction in gases and liquids, is introduced. The two sources of energy deposition, X-rays and neutrons, are included. The neutron energy deposition is determined by means of a general Monte Carlo code for neutron transport. The sequence of impact events is as follows. The X-ray prepulse arrives first, 17ns after it appears at the target surface. Then, in 70ns, the neutron pulse hits the lead film. The main X-ray pulse comes in approximately 320ns.

The impact of the X-ray prepulse is demonstrated in Fig.3, where the pressure distributions are plotted at various times. The pressure wave, generated by the X-ray

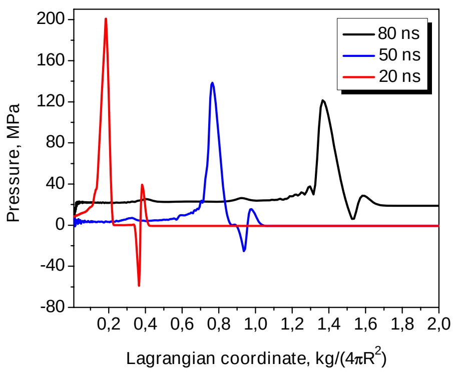

Fig.3.Pressure profiles in the liquid film at various times for the X-rays prepulse impact. R=5m.

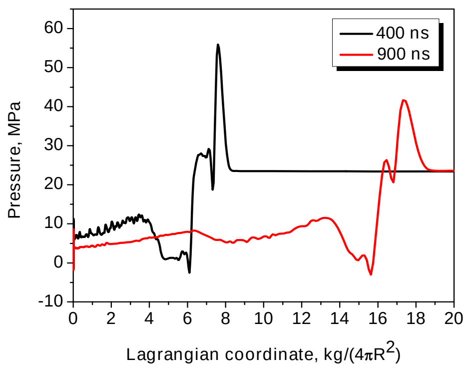

Fig.4. Pressure profiles in the liquid film at various times for the X-rays main pulse impact. R=5m.

prepulse, travels across the film. When neutron pulse arrives, the pressure rises practically uniformly across the film. Fig.4 illustrates the pressure evolution after the main X-ray pulse starts to be absorbed in the material unloaded by a release wave. It is seen that the amplitude of the emerging pressure wave does not exceed the pressure generated by the neutron pulse.

In Fig.5 the temperature and density distributions of the vapor layer at the liquid film are drawn at the time of 900ns. The effects of heating of the external part of the vapor layer by X-ray absorption, and of the heat conduction to the liquid surface are observed. The vaporization dynamics is presented in Fig.6. Here vaporization front velocity and evaporated mass are plotted for the sphere of 5m radius.

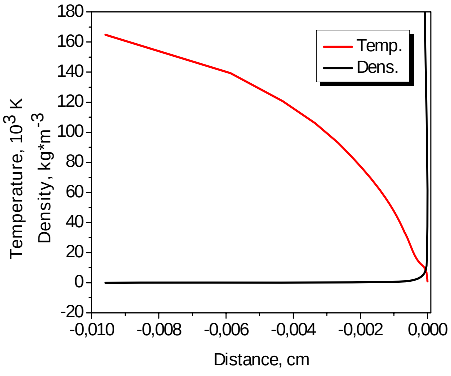

Fig.5.Temperature and density distributions in the vapor layer at the time of 900ns.

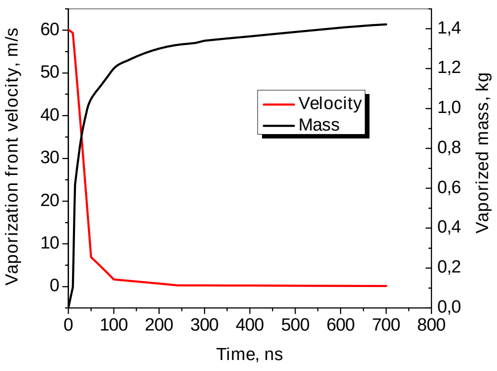

Fig.6.Time dependence of vaporization front velocity and evaporated mass of liquid.

The target fireball expansion. The fireball expansion is computed in the same 1D1T approximation as for the liquid film. The initial data are taken from the target output. At t=0 the target internal energy and the density are set constant and equal to 44.5MJ/g and 11.3g/cm^3 correspondingly. The velocity equals to zero. In Fig.7 the temperature profiles are drawn at various time moments. The pressure, temperature and velocity are shown in

Fig.8 at 55 μs, the time when the contact between the target fireball and the film target layer takes place. The characteristic parameters of the fireball were used for evaluation of vapor layer heating by the fireball high energy ions. The rate of ion energy losses in the vapor layer is estimated by Bethe-Bloch relationship as 20 GeV/g/cm^2. This is much less than the vapor layer thickness. Thus the vapor is superheated to the temperature of about 40eV and the resulting vaporization of the film amounts to 15kg.

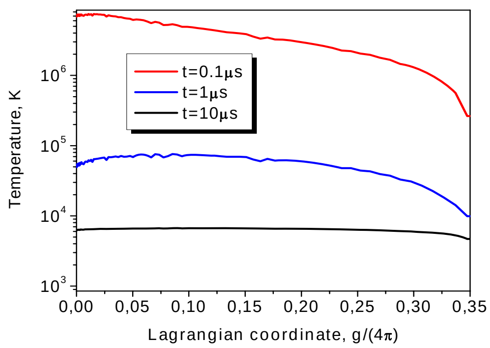

Fig.7.The temperature profiles in the fireball at various times, t=0,1; 1; 10 μs.

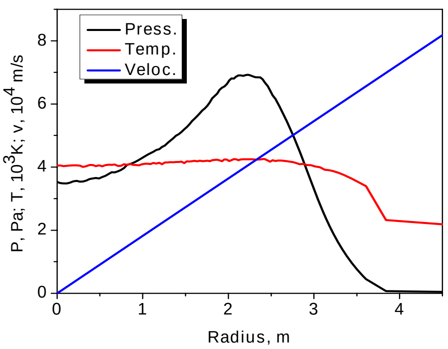

Fig.8.Distributions of pressure p, temperature T and velocity v in the fireball at 55 μs.

Conclusions. In heavy ion fusion a massive cylindrical target is a natural design option. This target produces relatively high energy of ion debris and a moderate X-ray flare. The X-ray temporary profile is characterized by a short intensive prepulse followed by a low-amplitude extended main pulse. The vapor layer generated by the prepulse shields the liquid film from the main X-ray pulse. This reduces substantially the X-ray impact on the protection film at the first wall. The impact of the target debris is also absorbed by the vapor layer, and reradiation from the vapor leads to revaporisation of the liquid film. Although the one-dimensional radiation-hydrodynamic simulation demonstrates effective fuel compression and burn, a confirmation of the target performance in 2D description is needed, for a more detailed design of the target. Another issue to be addressed is the coupled computation of interaction of the target debris, vapor layer and the liquid film.

REFERENCES

1. M.M.Basko, DEIRA. A1-D 3-T hydrodynamic code for simulating ICF targets driven by fast ion beams. Version 4, Institute for Theoretical and Experimental Physics, Moscow, 2001, p.44.
2. S.Medin, M.Basko, M.Churazov, P.Ivanov, D.Koshkarev, Yu.Orlov, A.Parshikov, B.Sharkov, V.Suslin, Power plant conceptual design for fast ignition heavy ion fusion, NIMA, v.544, 2005, pp.300-309.